Modeling static microstructure of shape memory alloy via Legendre wavelets collocation method

Xuan He[1,2], Haoyuan Du[1], Zixiang Ying[1], Linxiang Wang[1]* and Roderick Melnik[2]

[1]State Key Laboratory of Fluid Power and Mechatronic Systems, Zhejiang University, 310027, Hangzhou, China
[2]MS2Discovery Interdisciplinary Research Institute, Wilfrid Laurier University, Waterloo, ON N2L 3L5, Canada

E-mail: xuanhe@zju.edu.cn

Abstract. The static microstructures of square-to-rectangular phase transformations are modeled in the current paper. Governing equations are described by the static Navier equations. The analysis of the simulation has been finished via Legendre wavelets collocation method. Microstructure evolutions of both 2D and 1D shape memory alloy (SMA) are capture well with a certain boundary condition and given mechanical loadings.

1. Introduction

Shape memory alloys (SMA) are widely applied in industries due to its unique thermo-dynamical properties [1-3]. One of the famous effects of SMA, which is called the shape memory effect, is that the strain of SMA occurred in the martensite phase at low temperature will be recovered in the austenite phase at high temperature. Another famous effect is about elasticity beyond common sense. It is called pseudoelasticity that some phase transformations (austenite → martensite) happen under the external mechanical loadings with a certain range of temperature, and the transformation, as well as strain it caused, will be reversed without the loadings. These two effects are the major topic of the researcher's work. Many related studies are ultimately attributed to the researches of microstructure. The better understanding of microstructure we got, the better application of SMA we did.

One popular way to study microstructure is based on Landau free energy minimization [4-6], and such researches are attributed to the numerical solution of partial differential equations. Legendre wavelets method (LWM) is an emerging spectral method to solve such problems. LWM combines the advantage of both spectral method and wavelet method, and it is good at stability, high precision as well as good efficiency [7].

In the current paper, the static microstructure of SMA model is simulated via Legendre wavelets method at a certain temperature. The analysis of phase combinations in these situations is presented as well. The current paper is organized as follows. An introduction of Legendre wavelets is given in section.2. The model of SMA is presented in section.3. Finally, the simulations and analysis are discussed in section.4 and section.5. Concluding is given in section.6.

2. A mathematical model for SMA

Square-to-rectangular martensitic phase transformations are considered in the current paper, which can be treated as a simplified 2D analog of the cubic-to-tetragonal or tetragonal-to-orthorhombic phase transformations [8]. Considering the fundamental laws, energy balance and so on, the basic functions used

in the current paper are illustrated by static Navier equations as follows[8]:

$$\frac{\partial\sigma_{11}}{\partial x}+\frac{\partial\sigma_{21}}{\partial y}+f_x=0, \tag{1.a}$$

$$\frac{\partial\sigma_{12}}{\partial x}+\frac{\partial\sigma_{22}}{\partial y}+f_y=0, \tag{1.b}$$

where σ_{ij} is the stress tensor, and f_i is the mechanical loading in x_i direction.
The stress tensor can be given by the thermos-dynamical equilibrium conditions:

$$\sigma_{ij}=\frac{\delta\Psi(\Delta\theta,\varepsilon)}{\delta\varepsilon_{ij}}, \tag{2}$$

where ε_{ij} is the Cauchy-Lagrangian strain tensor which is given as follows:

$$\varepsilon_{ij}(x,t)=\frac{\frac{\partial u_i(x,t)}{\partial x_j}+\frac{\partial u_j(x,t)}{\partial x_i}}{2}, \tag{3}$$

where u_i is the displacement.
The free energy function $\Psi(\Delta\theta,\varepsilon)$ can be obtained by the Landau theory:

$$\Psi(\Delta\theta,\varepsilon)=\frac{a_1}{2}e_1^2+\frac{a_3}{2}e_3^2+F_l+F_g, \tag{4.a}$$

$$F_l=\frac{a_2}{2}\Delta\theta e_2^2-\frac{a_4}{4}e_2^4+\frac{a_6}{6}e_2^6, \tag{4.b}$$

$$F_g=\frac{k_g}{2}\left[\left(\frac{\partial e_2}{\partial x}\right)^2+\left(\frac{\partial e_2}{\partial y}\right)^2\right], \tag{4.c}$$

where e_1, e_2 and e_3 are the hydrostatic, deviatoric and shear strain respectively defined as $e_1=\frac{\varepsilon_{xx}+\varepsilon_{yy}}{\sqrt{2}}$,$e_2=\frac{\varepsilon_{xx}-\varepsilon_{yy}}{\sqrt{2}}$,$e_3=\frac{\varepsilon_{xy}+\varepsilon_{yx}}{2}$.

3. Numerical algorithm via Legendre wavelets

The simulation of nonlinear wave propagation based on a coupled system of PDEs is not a trivial task to solve the 2D situation. The choice of the algorithm will substantially affect the accuracy of the result. In the current paper, the Legendre wavelets method (LWM) is employed to simulation this hard task.

The wavelet methods can reduce calculation cost-effectively. The Legendre wavelets method(LWM) is originated from applying wavelets method to the mother function Legendre polynomials. The Legendre wavelets family retains the following form[9]:

$$\psi_{n_1,m_1,n_2,m_2}(x,y)=\begin{cases}A\cdot P_{m_1}(n_1')\cdot P_{m_2}(n_2'), & \frac{n_1-1}{2^{k_1-1}}\le x\le\frac{n_1}{2^{k_1-1}},\frac{n_2-1}{2^{k_2-1}}\le y\le\frac{n_2}{2^{k_2-1}}\\ 0, & \text{otherwise}\end{cases} \tag{5}$$

where $n_i'=2^{k_i}x-2n_i+1$ $m_i=0,1,...,M-1$, $n_i=1,2,3,...,2^{k-1}$, $A=\sqrt{(m_1+\frac{1}{2})(m_2+\frac{1}{2})}2^{\frac{k_1+k_2}{2}}$ is the coefficient for orthogonality. P_{m_i} are Legendre polynomials with order m_i on interval [-1,1].
Function $f(x,y)$ defined on interval [0, 1]×[0, 1] can be expanded as Legendre wavelets as follows:

$$f(x)=\sum_{n_1=1}^{\infty}\sum_{m_1=0}^{\infty}\sum_{n_2=0}^{\infty}\sum_{m_2=0}^{\infty}c_{n_1,m_1,n_2,m_2}\psi_{n_1,m_1,n_2,m_2}(x)=C^T\Psi(x). \tag{7.a}$$

here $c_{n,m}$ denoted the inner product of $f(x)$ and $\psi_{n,m}(x)$. If Eq.(5) is truncated, it can be rewritten as

$$f(x)=\sum_{n_1=1}^{2^{k-1}}\sum_{n_2=1}^{2^{k-1}}\sum_{m_1=0}^{M-1}\sum_{m_2=0}^{M-1}c_{n_1,m_1,n_2,m_2}\psi_{n_1,m_1,n_2,m_2}(x)=C^T\Psi(x), \tag{7.b}$$

The vector C in Eq. (7) is called the spectral space coefficient, and C is the only data needed in the following calculations.

3.1. Operational matrix of derivatives

In the present paper, due to the properties of Legendre polynomials, the calculation of derivatives in this method can be obtained in the matrix form [10]:

$$\frac{d\Psi(x,y)}{dx}=D_x\Psi(x,y), \tag{8}$$

where D_x is a $2^kM2^{k'}M'\times 2^kM2^{k'}M'$ derivative matrix defined as follows:

$$D_x = \begin{pmatrix} F & 0 & \cdots & 0 \\ 0 & F & & 0 \\ \vdots & & \ddots & \vdots \\ 0 & 0 & \cdots & F \end{pmatrix}, \tag{9}$$

where F is a $M2^{k'}M' \times M2^{k'}M$' matrix which is defined as follow:

$$F_{r,s} = \begin{cases} 2^{k+1}\sqrt{(2r-1)(2s-1)}\,, & r = 2,...,M,\ S = 1,...,r-1, \text{ and } (r+s) \text{ odd}, \\ 0, & \text{otherwise.} \end{cases} \tag{10}$$

$$\frac{d\Psi(x,y)}{dy} = D_y\Psi(x,y),$$

$$D_y = \begin{pmatrix} D & 0 & \cdots & 0 \\ 0 & D & & 0 \\ \vdots & & \ddots & \vdots \\ 0 & 0 & \cdots & D \end{pmatrix}$$

$$D = \begin{pmatrix} FF & 0 & \cdots & 0 \\ 0 & FF & & 0 \\ \vdots & & \ddots & \vdots \\ 0 & 0 & \cdots & FF \end{pmatrix}$$

where D is a $M' \times M'$ matrix. FF is a $M' \times M$' matrix which is defined as follows:

$$FF_{r,s} = \begin{cases} 2^{k+1}\sqrt{(2r-1)(2s-1)}\,, & r = 2,...,M,\ S = 1,...,r-1, \text{ and } (r+s) \text{ odd}, \\ 0, & \text{otherwise.} \end{cases}$$

The calculation of derivatives in the spectral space can be easily obtained by multiply spectral space coefficient C and derivative matrix D_x and D_y.

3.2. Numerical algorithm

Above all, the governing system is described as follows:

$$\frac{\partial\sigma_{11}}{\partial x} + \frac{\partial\sigma_{21}}{\partial y} + f_x = 0, \tag{11.a}$$

$$\frac{\partial\sigma_{12}}{\partial x} + \frac{\partial\sigma_{22}}{\partial y} + f_y = 0, \tag{11.b}$$

$$\sigma_{11} = \frac{\sqrt{2}}{2}\left(a_1e_1 + a_2\Delta\theta e_2 - a_4e_2^3 + a_6e_2^5 - k_g\nabla^2e_2\right), \tag{11.c}$$

$$\sigma_{12} = \sigma_{21} = \frac{1}{2}a_3e_3, \tag{11.d}$$

$$\sigma_{22} = \frac{\sqrt{2}}{2}\left(a_1e_1 - a_2\Delta\theta e_2 + a_4e_2^3 - a_6e_2^5 + k_g\nabla^2e_2\right), \tag{11.e}$$

The boundary condition can be described as :

$u_i = 0$, $\frac{\partial u_j}{\partial x_i} = 0$ at the boundary area of x_i direction.

Moving to the time discretization procedure, system(11) can be rewritten as follows:

$$LU + N(x,y,U) = 0, \tag{12}$$

where L is the matrix of the linear operator, N is the matrix of the nonlinear operator and $U = [u_x,u_y]^T$.

This system is solved by using the θ weight formula as follows:

$$\theta LU^{n+1} + (1-\theta)LU^n + N(t,x,U^n) = 0, \tag{13}$$

where n is the current time layer.

Considering the 1-D static situation, the Eq.(11) can be recast as :

$$a_2\Delta\theta\frac{\partial^2u}{\partial x^2} + a_4\left(\frac{\partial u}{\partial x}\right)^2\frac{\partial^2u}{\partial x^2} + a_6\left(\frac{\partial u}{\partial x}\right)^4\frac{\partial^2u}{\partial x^2} - k_g\frac{\partial^4u}{\partial x^4} + f = 0\,, \tag{14}$$

with the same boundary conditions:

$u(0,t) = 0, \quad u(L) = 0,$

$u_{xx}(0,t) = 0, \quad u_{xx}(L,t) = 0.$

4. Numerical simulation

The numerical experiments data in the current paper were published in [11], which were gotten by

$Au_{23}Cu_{30}Zn_{47}$ materials:

$a_2 = 480\mathrm{g/(ms^2cmK)}$,$a_4 = 6 \times 10^6\mathrm{g/(ms^2cmK)}$,
$a_6 = 4.5 \times 10^8\mathrm{g/(ms^2cmK)}$,
$\theta_0 = 208\mathrm{k}$,
$\rho = 11.1\mathrm{g/cm^3}$,$c_v = 29\mathrm{g/(ms^2cmK)}$.

All the simulations were taken in the Matlab2015a.

4.1. Dimensionless form of the governing equations

The dimensionless form applied in the current can be referred to as the strategy in Ref. [12]:

4.2. Simulation results of 1-D SMA

In this section, the simulation was performed by the situation with $k = 5$ and $M = 6$ in section 3. The dimensionless form of the governing equations can be gotten from formula(14):

$$\sigma_{\tilde{x}} = \frac{\partial^4 \tilde{u}}{\partial \tilde{x}^4} - \tilde{f}, \qquad \sigma = \widetilde{k_1}\tilde{\varepsilon} + \tilde{\varepsilon}^3 + \tilde{\varepsilon}^5, \tag{15}$$

where $\widetilde{k_1}$ =0.192, $\tilde{f} = 0.4$, $\tilde{\varepsilon} = \frac{\partial \tilde{u}}{\partial \tilde{x}}$.

In this experiment, the temperature was set to $240\mathrm{K}$. Thus, the initial condition should begin from the austenitic phase:

$$\widetilde{u_0(x)} = 0. \tag{16}$$

Newton method was applied to complete this 1D simulation with the derivative matrix in section3.1. Fig.1(left) shows the figure of displacement $\tilde{u}$. Fig.1(right) shows the figure of strain $\tilde{\varepsilon}$. Under this mechanical loading, the simulation shows that the rod has finally finished the phase transformation into the martensite phase. And the results are in line with expectations.

4.3. Simulation results of 2-D SMA

In this section, the simulation was performed in an SMA film. The time stepsize in this experiment was set to $\Delta\tilde{t} = 1 \times 10^{-4}$. The initial value is given as a disordered martensite phase.

The mechanical loading which is time-varying is defined as

$$f_x = 500, \tag{17.a}$$
$$f_y = 500, \tag{17.b}$$

Under this mechanical loading, the SMA film should be switching between the martensite phase and the austenite phase. In this section, we set the temperature at $210\mathrm{K}$. Both the mechanical and temperature conditions make sure that only the martensite phase exists. And the free energy function here has two local minima which correspond to two martensites. The simulation results are present in Fig.2. It is shown that the initial disordered martensite phase is rearranged into the twins martensite phase ordered. Thus, the phase combinations are caused by the applied mechanical loading. Stress-induced phase combinations are captured well in this section.

5. Conclusion

In the current paper, an isothermal model has been proposed to simulate the static microstructure of SMA. The Microstructure evolutions in both 1D and 2D systems have been simulated via Legendre wavelets method successfully. The numerical algorithm for Legendre wavelets method to solve the partial differential equation has been described in the current paper. The simulation ability of LWM is shown.

References

[1] Mohd Jani J, Leary M, Subic A, et al. A review of shape memory alloy research, applications and opportunities[J]. Materials & Design, 2014, 56:1078-1113.

[2] Humbeeck J V. Non-medical applications of shape memory alloys[J]. Materials Science & Engineering A (Structural Materials, Properties, Microstructure and Processing), 1999,

273-275(none):134-148.

[3] Biesiekierski A, Wang J, Gepreel A H, et al. A new look at biomedical Ti-based shape memory alloys[J]. Acta biomaterialia, 2012, 8(5):1661-1669.

[4] L.X. Wang, R.V.N. Melnik, Simulation of phase combinations in shape memory alloys patches by hybrid optimization methods[J]. Applied Numerical Mathematics, 2008, 58(4):511-524.

[5] L.X. Wang, R.V.N. Melnik, Thermo-mechanical wave propagation in shape memory alloy rod with phase transformations, Mechanics of Advanced Materials and Structures, 2007, 14 (8):665-676.

[6] L.X. Wang, R.V.N. Melnik, Numerical model for vibration damping resulting from the first order phase transformations, Applied Mathematical Modelling, 2007, 31:2008-2018.

[7] Xuan He, Zheng Tong, Haoyuan Du, Dan Wang, Linxiang Wang and Roderick Melnik. Modeling microstructure evolution in shape memory alloy rods via Legendre wavelets collocation method. Journal of Materials Science. (2019) 54:14400-14413.

[8] Wang L X, Melnik R V N. Mechanically induced phase combination in shape memory alloys by Chebyshev collocation methods[J]. Materials Science & Engineering A (Structural Materials, Properties, Microstructure and Processing), 2006, 438-440(none):427-430.

[9] M. Razzaghi, S. Yousefi, Legendre wavelets method for the solution of nonlinear problems in the calculus of variations, Mathematical and Computer Modelling, 34.1–2,(2001), P 45-54,

[10] F. Mohammadi, M.M. Hosseini, A new Legendre wavelet operational matrix of derivative and its applications in solving the singular ordinary differential equations, Journal of the Franklin Institute, 348.8 (2011), p.1787-1796.

[11] L.X. Wang, R.V.N. Melnik, Finite volume analysis of nonlinear thermo-mechanical dynamics of shape memory alloys, Heat Mass Transfer (2007) 43:535–546

[12] Dhote, R. P., Gomez, H., Melnik, R. N. V., & Zu, J. (2015). 3D coupled thermo-mechanical phase-field modeling of shape memory alloy dynamics via isogeometric analysis. Computers & Structures, 154, 48–58.

Acknowledgments
This work has been supported by the National Natural Science Foundation of China (Grant No.51575478 and Grant No.61571007), the National Sciences and Engineering Research Council (NSERC) of Canada, and the Canada Research Chair Program.

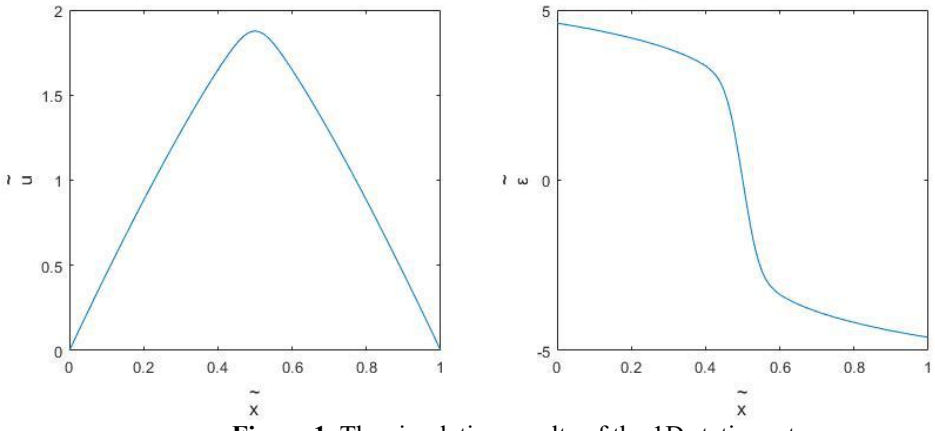

Figure 1. The simulation results of the 1D static system.

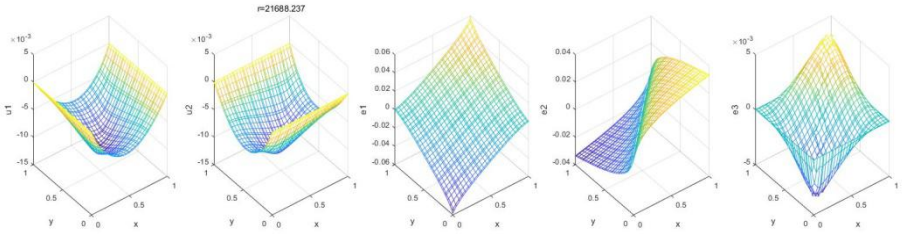

Figure 2. The simulation result of the 2D static system.